



# The Packaging Regions of G1-Like PB2 Gene Contribute to Improving the Survival Advantage of Genotype S H9N2 Virus in China

Xiuli Li<sup>1</sup>, Ying Zhao<sup>1</sup>, Shumiao Qiao<sup>1</sup>, Min Gu<sup>1</sup>, Ruyi Gao<sup>1</sup>, Zhichuang Ge<sup>1</sup>, Xiulong Xu<sup>2,3,4</sup>, Xiaoquan Wang<sup>1</sup>, Jing Ma<sup>1</sup>, Jiao Hu<sup>1</sup>, Shunlin Hu<sup>1</sup>, Xiaowen Liu<sup>1</sup>, Sujuan Chen<sup>1</sup>, Daxin Peng<sup>1</sup>, Xinan Jiao<sup>2,3,5</sup> and Xiufan Liu<sup>1,5\*</sup>

<sup>1</sup> Animal Infectious Disease Laboratory, School of Veterinary Medicine, Yangzhou University, Yangzhou, China, <sup>2</sup> College of Veterinary Medicine, Institute of Comparative Medicine, Yangzhou University, Yangzhou, China, <sup>3</sup> Yangzhou University Joint International Research Laboratory of Agriculture and Agri-Product Safety of Ministry of Education of China, Institutes of Agricultural Science and Technology Development, Yangzhou University, Yangzhou, China, <sup>4</sup> Jiangsu Co-innovation Center for Prevention and Control of Important Animal Infectious Diseases and Zoonosis, Yangzhou University, Yangzhou, China, <sup>5</sup> Jiangsu Key Laboratory of Zoonosis, Yangzhou University, Yangzhou, China

## OPEN ACCESS

### Edited by:

Akio Adachi,  
Kansai Medical University, Japan

### Reviewed by:

Juan Pu,  
China Agricultural University, China  
Seiya Yamayoshi,  
University of Tokyo, Japan  
Jun Ji,  
Nanyang Normal University, China

### \*Correspondence:

Xiufan Liu  
xliu@yzu.edu.cn

### Specialty section:

This article was submitted to  
Virology,  
a section of the journal  
Frontiers in Microbiology

**Received:** 18 January 2021

**Accepted:** 25 March 2021

**Published:** 21 April 2021

### Citation:

Li X, Zhao Y, Qiao S, Gu M, Gao R, Ge Z, Xu X, Wang X, Ma J, Hu J, Hu S, Liu X, Chen S, Peng D, Jiao X and Liu X (2021) The Packaging Regions of G1-Like PB2 Gene Contribute to Improving the Survival Advantage of Genotype S H9N2 Virus in China. *Front. Microbiol.* 12:655057. doi: 10.3389/fmicb.2021.655057

The genotype S (G57) H9N2 virus, which first emerged in 2007 with the substitution of the G1-like PB2 gene for F98-like ones, has become the predominant genotype in the past 10 years. However, whether this substitution plays a role in the fitness of genotype S H9N2 viruses remains unknown. Comparison of the PB2 genes of F98-like and G1-like viruses revealed a close homology in amino acid sequences but great variations at nucleotide levels. We then determined if the packaging region, a unique sequence in each segment utilized for the assembly of the vRNA into virions, played a role in the fitness of the S genotype. The chimeric H9N2 virus with PB2 segments of the G1-like packaging regions significantly increased viral protein levels and polymerase activity. Substituting the packaging regions in the two terminals of F98-like PB2 with the sequence of G1-like further improved its competitive advantage. Substitution of the packaging regions of F98-like PB2 with those of G1-like sequences increased the infectivity of the chimeric virus in the lungs and brains of chicken at 3 days post infection (dpi) and extended the lengths of virus shedding time. Our study suggests that the packaging regions of the G1-like PB2 gene contribute to improve the survival advantage of the genotype S H9N2 virus in China.

**Keywords:** genotype S H9N2 virus, PB2 gene, packaging region, virus replication, competitive advantage

## INTRODUCTION

H9N2 viruses have evolved into multiple genotypes (A-W) since its first emergence in China in 1994. These genotypes are divided into five lineages including A/chicken/Beijing/1/1994 (BJ94-like), A/duck/Hong Kong/Y280/1997 (Y280-like), A/quail/HongKong/G1/1997 (G1-like), A/duck/HongKong/Y439/1997 (Y439-like), and A/chicken/Shanghai/F/1998 (F98-like) (Huang et al., 2010; Zhang et al., 2012; Liu et al., 2016; Gu et al., 2017). More than one genotype may

circulate simultaneously in one region (Gu et al., 2017). Among a few genotypes prevalent in China before 1999, the BJ94-like series is the predominant one (Gu et al., 2017; Li et al., 2017). Since then, various reassortments have significantly increased the number of the genotypes of H9N2 viruses, whereas the genetic diversity of H9N2 viruses decreased since 2006. The genotype S (G57) H9N2 viruses generated through the reassortment of F98-like viruses by substituting their M and PB2 genes with those of the G1-like emerged first in 2007 and have become predominant in China since 2010s (Gu et al., 2014, 2017). Although the roles of G1-like M and PB2 reassortment in H7N9 and H5Nx viruses have been well characterized (Hao et al., 2019, 2020), the impact of G1-like PB2 on H9N2 virus fitness is yet to be investigated.

The highly selective genome packaging of influenza A viruses relies on complex RNA-RNA or RNA-protein interactions (Liang et al., 2005; Fournier et al., 2012). The specific structures of each vRNA that contribute to the packaging of the vRNA have been identified as packaging signals (Liang et al., 2005; Ozawa et al., 2009; Cobbin et al., 2014; Zhao et al., 2014; Gilbertson et al., 2016). The untranslated regions as well as 300-nt of the coding sequences of PB2 vRNA at both ends are essential for the efficient genome packaging of the WSN virus (Liang et al., 2005, 2008; Muramoto et al., 2006). Recently, stem-loop structures in the terminal packaging sequences in both M and PB2 vRNA are found to be crucial for the infectivity of viruses and the assembly of infectious virion particles (Kobayashi et al., 2016, 2018; Spronken et al., 2017). Our present study aimed at determining if the G1-like PB2 packaging regions contributed to the dominance of genotype S H9N2 viruses. Here we report that substituting the packaging region of F98-like with that of G1-like PB2 led to increased PB2 expression and the production of infectious virus *in vitro* and *in vivo*. Our study unveils a previously unrecognized role of the packaging regions in genotype S H9N2 virus evolution in China.

## MATERIALS AND METHODS

### Ethics Statement

This study was carried out in strict accordance with the recommendations in the Guide for the Care and Use of Laboratory Animals of the Ministry of Science and Technology of the People's Republic of China. All animal experiments were approved by the Jiangsu Administrative Committee for Laboratory Animals (Permission number: SYXK-SU-2017-0007), and by the Institutional Biosafety Committee of Yangzhou University and complied with the guidelines of Jiangsu laboratory animal welfare and ethics of Jiangsu Administrative Committee of Laboratory Animals.

### Phylogenetic Analysis of All Segments of H9N2 Viruses

The sequences of PB2 of all H9N2 AIVs isolated between 1996 and 2019 were downloaded from the EpiFlu Database (GISAIID): <https://www.gisaid.org/registration/terms-of-use/>. The Isolate

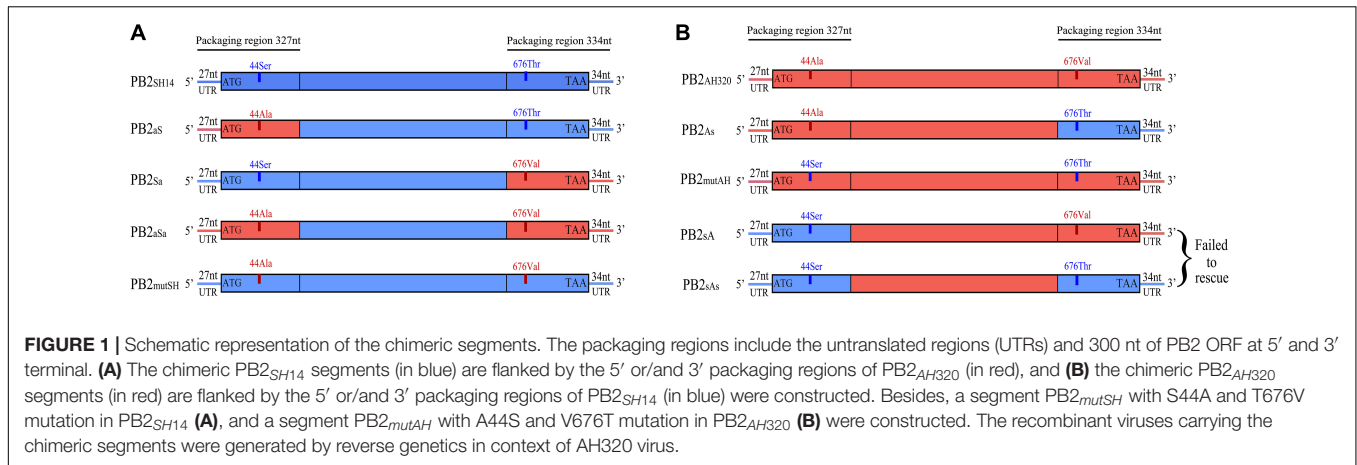
IDs can be found in **Supplementary Dataset 1**. Each segment was aligned using PhyloSuite, corrected frame shift errors, and then translated to amino acid sequences with mega 5.0. Phylogenetic tree reconstruction and mean group distance were carried out using the Mega 5.0 software with the neighbor-joining method. The robustness of the statistical support for the tree branch was determined by 1,000 bootstrap replicates.

### Minigenome Polymerase Activity Assay

A set of plasmids were generated on the pHW2000 backbone, carrying each segment of A/Chicken/Anhui/AH320/2016 (genotype S H9N2), F98-like PB2 gene from A/Chicken/Shanghai/14/2001 (H9N2), and chimeric PB2 segments, respectively. 293T cells were transfected with 300 ng firefly luciferase reporter, 30 ng of the control pRL-TK vector, which expresses the Renilla luciferase, and 300 ng each of PB1, PA, NP and PB2 plasmids shown in **Figure 1** (Salomon et al., 2006; Marjuki et al., 2007; McAuley et al., 2010). After 48 h, cell extracts were analyzed for luciferase activity by using Dual-Luciferase Reporter assay system (Promega). The results were expressed as the relative activity compared to that in the reaction containing the PB2<sub>SH14</sub> or PB2<sub>AH320</sub> plasmid for each experiment. All results were the means  $\pm$  SD from three independent experiments.

### Determination of Protein Expression and RNA Synthesis Activity

The protein expression and RNA synthesis were quantified by Western blot and real-time RT-PCR in a four-plasmid expression system or infection conditions, respectively. (i) Triplicate wells of 293T cells were transfected with four plasmids, including PB1, PA, NP, and the chimeric PB2 segment showed in **Figure 1**, each at 300 ng concentration (Liang et al., 2005, 2008). (ii) Triplicate wells of MDCK cells were infected with each plaque purified virus at a multiplicity of infection of 1 MOI of each virus as described previously (White et al., 2017). Briefly, the infected cells were inoculated at 4°C for 45 min to allow for viruses attachment. Subsequently, the inoculum was removed, the cells were washed 3 times with cold PBS, and warm opti-MEM was added. After a 3 h incubation period at 37°C, the medium was removed and replaced with the opti-MEM containing 50 mmol ammonium chloride. The absence of TPCK-treated trypsin and the presence of NH<sub>4</sub>Cl restrict the infection to a single cycle. Forty-eight hours post-transfection/post-infection, the above transfected/or infected cells and the infected supernatants were harvested for subsequent western-blot or RNA extraction. The quantitative real-time RT-PCR was conducted with differences in the primers used for RT and real-time PCR. For the detection of mRNA, vRNA and cRNA, the oligo (dT) primer, the uni-12 primer (5'-AGCAAAGCAGG-3') and the uni-13 primer (5'-AGTAGAAACAAGG-3') were used to generate cDNAs with 500 ng of total RNA from cell sample or 200 ng of total RNA from supernatant sample, respectively. The gene-specific primers



for the real-time PCR were 5'-TTGCTCCTTTAATGGTGGC-3' and 5'-TCCCAGCAGGTCCCTTG-3' for all PB2 genes, and the probes were VIC-TTGTCCTCCAGCTACTGG-MGB for the PB2 genes mutated from PB2<sub>AH320</sub> backbone and 5'-FAM-CGGTAGCAGGTGGAACAA-MGB-3' for the PB2 genes mutated from PB2<sub>SH14</sub> backbone. The PB2 RNA levels shown were as log<sub>10</sub> of copy numbers.

## Co-infection of MDCK Cells With Reassortant Viruses

Triplicate wells of MDCK cells were coinfecting 1 MOI for each virus. The viruses containing the mutants from PB2<sub>SH14</sub> gene were coinfecting with P-WT-AH320 virus, and the viruses containing the mutants from PB2<sub>AH320</sub> gene were coinfecting with P-AH320-PB2<sub>SH14</sub> virus. As described above, the medium was replaced with opti-MEM containing 50 mmol NH<sub>4</sub>CL to ensure a single cycle of viral replication. At 48 hpi, the infected cells and supernatants were collected for RNA extraction, and the RNA levels were detected with the quantitative real-time RT-PCR as described above.

Every experiment was run in triplicate wells and repeated at least twice.

## Animal Experiment

Eight 5 weeks old SPF white leghorn chickens were inoculated intraocularly with 10<sup>6</sup> 50% egg infective doses (EID<sub>50</sub>) of each plaque purified mutant viruses. Three chickens were euthanized by CO<sub>2</sub> asphyxiation for each group at 3 and 5 dpi, and lungs and brains were collected for virus titration. At 1, 3, 5, and 7 dpi, oropharyngeal and cloacal swabs from five chickens of each group were taken for the detection of viral shedding.

## Statistical Analysis

Statistical analyses were conducted by using SAS software, version 9.2 (SAS Institute). Statistically significant differences between the number of the copies of G1-like PB2 and F98-like PB2 genes were analysed by using Duncan's multiple range test in ANOVA. Differences were considered significant at  $P < 0.05$ .

## RESULTS

### Abundant Synonymous Mutations Between G1-Like PB2 and F98-Like PB2

All available PB2 sequences of H9N2 AIV during 1996–2019 were downloaded from the EpiFlu Database (GISAID): <https://www.gisaid.org/registration/terms-of-use/>. Phylogenetic analysis revealed that the PB2 genes of H9N2 AIV in China are clustered into five independent branches: that is BJ94-like, wild-waterfowl-like, F98-like, G1-like (2006) (which spread prior to 2006) and G1-like that spread since 2007 (**Supplementary Figure 1**). The mean group distance of each segment is shown as **Supplementary Table 1**. Nucleotide variations among PB2 nucleotides are much higher than the amino acid sequences of PB2 protein. This suggests that synonymous mutations have occurred during the evolution of the PB2 gene. The conservation of PB2 amino acid sequences may be required for maintaining the structure and function of PB2 polymerase (Zhao et al., 2011).

### Generation of Reassortant Viruses by Reverse Genetics

The coding and non-coding regions in the two ends of the PB2 gene are involved in genome incorporation into the virion of WSN virus (Liang et al., 2005, 2008; Muramoto et al., 2006). To investigate the effect of PB2 nucleotide variations on the adaptability of H9N2 virus, we constructed chimeric PB2 segments by exchanging the packaging regions of PB2<sub>SH14</sub> (F98-like) and PB2<sub>AH320</sub> (G1-like) genes (**Figure 1**). There are two amino acid differences at position 44 and 676 in the region of the packaging region between PB2<sub>SH14</sub> and PB2<sub>AH320</sub> genes. We constructed a PB2<sub>mutSH</sub> segment with S44A and T676V mutation in PB2<sub>SH14</sub> (**Figure 1A**), and a PB2<sub>mutAH</sub> segment with A44S and V676T mutation in PB2<sub>AH320</sub> gene (**Figure 1B**). Eight reassortant H9N2 viruses (AH320-PB2<sub>SH14</sub>, AH320-PB2<sub>aS</sub>, AH320-PB2<sub>sA</sub>, AH320-PB2<sub>sSa</sub>, AH320-PB2<sub>mutSH</sub>, WT-AH320, AH320-PB2<sub>aS</sub>, and AH320-PB2<sub>mutAH</sub>) harboring the mutant PB2 segment mentioned above were successfully rescued in the background of AH320 virus.

However, the attempt to generate AH320-PB2<sub>sA</sub> and AH320-PB2<sub>sAs</sub> reassortants was not successful. By serial plaque purification, P-AH320-PB2<sub>SH14</sub>, P-AH320-PB2<sub>aS</sub>, P-AH320-PB2<sub>sA</sub>, P-AH320-PB2<sub>aSa</sub>, P-AH320-PB2<sub>mutSH</sub>, P-WT-AH320, P-AH320-PB2<sub>As</sub>, and P-AH320-PB2<sub>mutAH</sub> viruses were obtained from the rescued viruses.

### Chimeric PB2 Segments Carrying G1-Like Packaging Regions Increase PB2 Expression and Polymerase Activity

To determine the relative contribution of PB2 vRNA sequences to the prevalence of genotype S H9N2 viruses, we constructed chimeric PB2 segments by exchanging the packaging regions of PB2<sub>SH14</sub> and PB2<sub>AH320</sub> genes (Figure 1). We then examined the polymerase activity of these mutant PB2 genes using a minigenome system in a constant AH320 background. As shown in Figure 2A, substituting 5' or/and 3' terminal packaging regions of PB2<sub>SH14</sub> with PB2<sub>AH320</sub> sequences increased the viral polymerase activity at different levels. However, the amino acid mutation of PB2<sub>SH14</sub> in 44 and 676 positions did not significantly affect the polymerase activity in the AH320 background. Correspondingly, the RNA and protein levels of the chimeric segments were significantly elevated in most mutant segments based on PB2<sub>SH14</sub> (Figures 2C,E). However, replacing the packaging region at the 5' end of PB2<sub>SH14</sub> with the G1-like sequence of PB2<sub>AH320</sub> had limited effect on its RNA synthesis (Figure 2E, PB2<sub>aS</sub>).

The G1-like packaging regions of PB2<sub>AH320</sub> were reciprocally substituted by the F98-like sequences (Figure 1B). Except PB2<sub>As</sub>, all other mutant PB2 genes reduced viral polymerase activity. PB2<sub>sA</sub> and PB2<sub>sAs</sub> decreased viral polymerase activity most effectively (Figure 2B). The levels of PB2<sub>As</sub> and PB2<sub>mutAH</sub> proteins did not significantly decrease. However, the levels of PB2<sub>sA</sub> and PB2<sub>sAs</sub> proteins were much lower than their parental PB2<sub>AH320</sub> gene (Figure 2D). Failure to produce reassortant viruses AH320-PB2<sub>sA</sub> and AH320-PB2<sub>sAs</sub> was likely due to the poor expression of their proteins. Besides, some studies reported that the secondary structure of AIV segments rather than their wild type nucleotide sequences may play a more important role in the incorporation of vRNA process (Dadonaite et al., 2019). The vRNA structure alteration of PB2 segment caused by PB2<sub>sA</sub> and PB2<sub>sAs</sub> may disturb the redundant and plastic network of RNA-RNA and potentially RNA-nucleoprotein interactions which are believed to be crucial for AIV genome packaging (Liang et al., 2005; Muramoto et al., 2006; Fournier et al., 2012; Bolte et al., 2019). The substitution of the packaging regions in PB2<sub>AH320</sub> only slightly decreased RNA levels (Figure 2F). Consistently, the sequence exchange at 5' end of PB2<sub>AH320</sub> (PB2<sub>sA</sub> segment) had little impact on RNA synthesis, either.

The observation that mRNA synthesis level of several mutants was inconsistent with their protein expression may be related to the post-transcriptional processing, regulation and translation of PB2 gene (Chen et al., 2002; Griffin et al., 2002).

### The Packaging Regions of G1-Like PB2 Improves the Production of Infectious Virus Particles

It's reported that non-infectious viruses are usually associated with a decrease in PFU/HAU or TCID<sub>50</sub>/HAU ratio (Xue et al., 2016; Bolte et al., 2019). In our study, the virus titers and their infectious particles in the rescued virus stock were measured by the HA test [hemagglutination units (HAU)] and the TCID<sub>50</sub> values, respectively (Carter and Mahy, 1982a,b; Xue et al., 2016). The percent of infectious particles were calculated based on the ratio of TCID<sub>50</sub> to HAU. As shown in Table 1, the mutant virus of AH320-PB2<sub>SH14</sub> gave a lowest TCID<sub>50</sub>/HAU ratio of 87 among the reassortant viruses. The TCID<sub>50</sub>/HAU ratio of the mutant viruses that replaced the packaging regions of PB2<sub>SH14</sub> with G1-like sequences of PB2<sub>AH320</sub> gene were improved to the range from 405 to 873. In contrast, the TCID<sub>50</sub>/HAU ratios of mutant viruses AH320-PB2<sub>As</sub> and AH320-PB2<sub>mutAH</sub> were 582 and 8,734, which were much lower than that of their parental WT-AH320 virus.

These data demonstrated that the rescued viruses contained non-infectious viral particles, and the viruses harboring the packaging regions of F/98-like PB2 gene produced non-infectious viral particles more abundantly than that of G1-like packaging regions. To minimize contamination of the rescued virus, all the viruses were purified by a series of plaque experiments (Xue et al., 2016). As expected, the TCID<sub>50</sub>/HAU ratio was elevated (Table 1), indicating the increase of infectious viral particles in rescued viruses.

To further explore the effects of PB2 packaging regions on the production of virus particles, the TCID<sub>50</sub>/HAU ratio of the mutant virus in the conditioned media of MDCK cells at 48 hpi were calculated. Compared to AH320-PB2<sub>SH14</sub> virus, the number of progeny virus particles and the proportion of infectious virus particles were improved by replacing the packaging regions of PB2<sub>SH14</sub> with that of PB2<sub>AH320</sub> gene (Figure 3A). The replacement of the packaging region at 3' end of PB2<sub>SH14</sub> had a greater impact on the generation of virus particles than that at the 5' end. Replacing the packaging regions of PB2<sub>SH14</sub> at both ends increased the production of infectious virus particles to the levels equivalent to the WT-AH320 virus (Figure 3B, AH320-PB2<sub>aSa</sub>). Substitution of 3'-terminal packaging region of the PB2<sub>AH320</sub> gene reduced the proportion of infectious virus particles to a level similarly to that of AH320-PB2<sub>SH14</sub> virus (Figure 3A, AH320-PB2<sub>As</sub>). While amino acid substitutions at 44 and 676 positions in PB2<sub>SH14</sub> increased the production of infectious virus (Figure 3A), but had mild effect in PB2<sub>AH320</sub> (Figure 3B).

### The Packaging Regions of G1-like PB2 Gene Increase H9N2 Virus Replication

We next determined the growth curve of plaque-purified viruses. As shown in Figure 4A, P-AH320-PB2<sub>aS</sub> and P-AH320-PB2<sub>sA</sub> viruses that substituted the packaging region of PB2<sub>SH14</sub> at either end replicated similarly fast as did P-AH320-PB2<sub>SH14</sub> (Figure 4A). While replacing the packaging regions of PB2<sub>SH14</sub> at both ends with that of PB2<sub>AH320</sub> (P-AH320-PB2<sub>aSa</sub> virus)

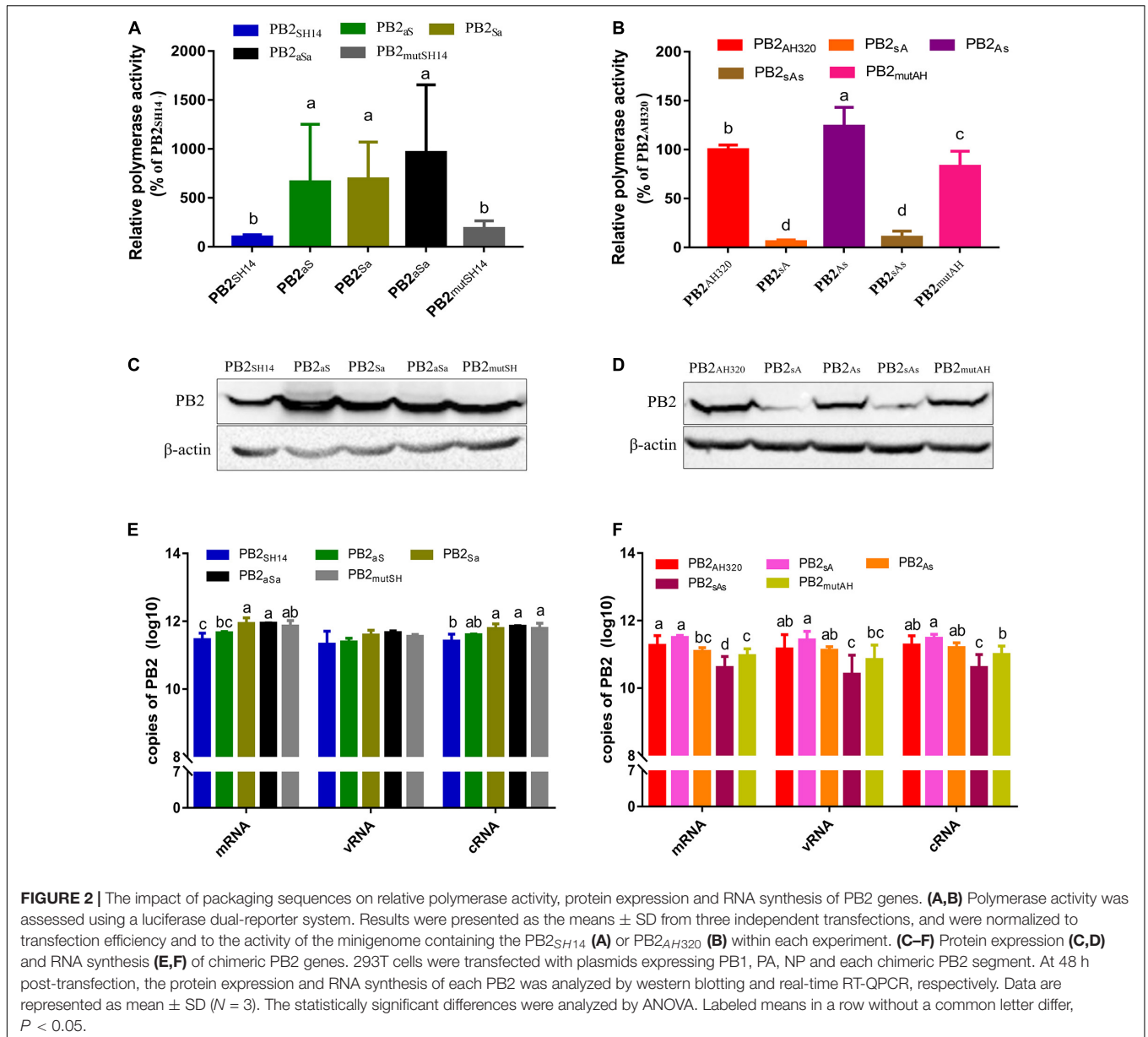
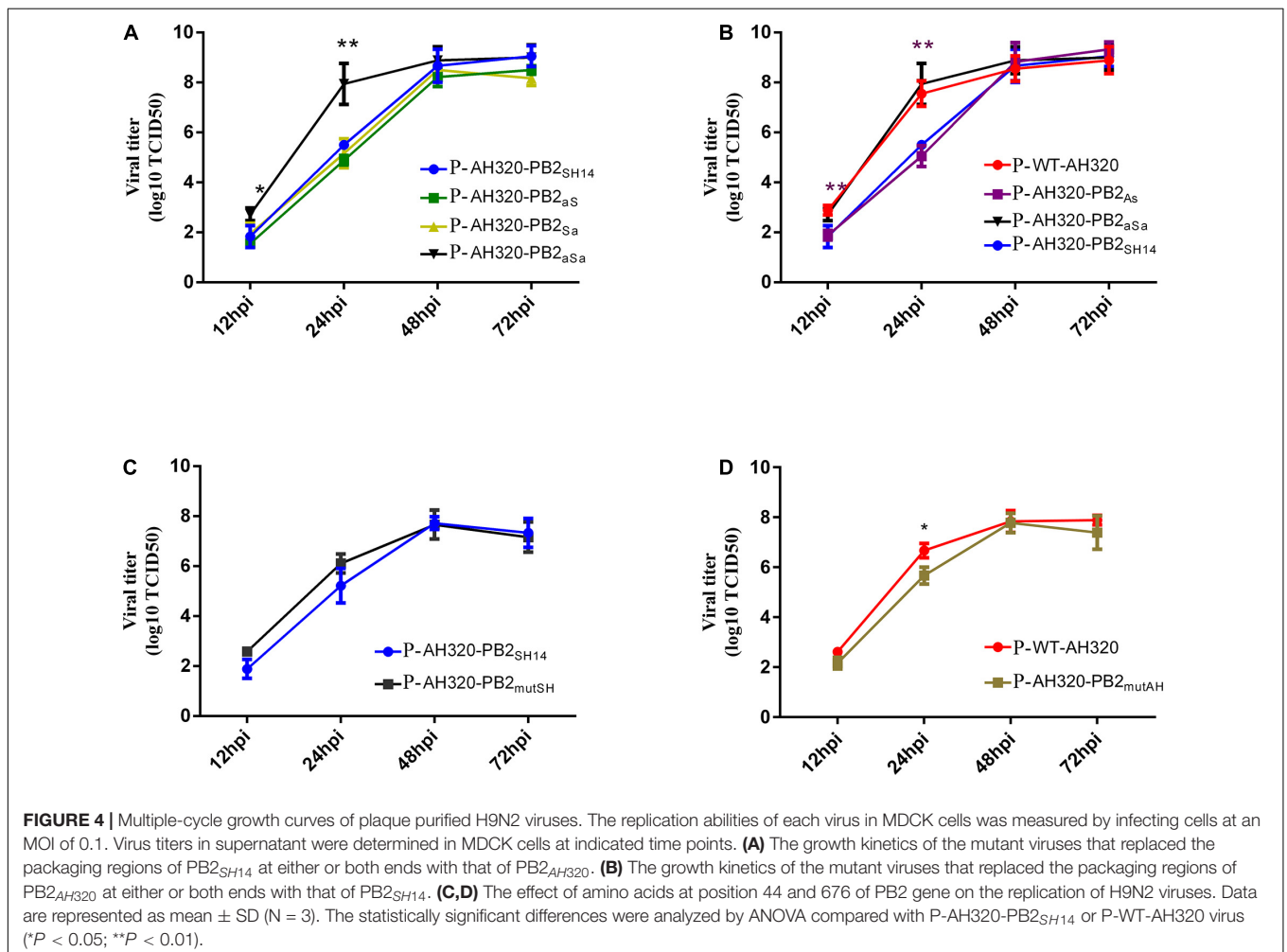
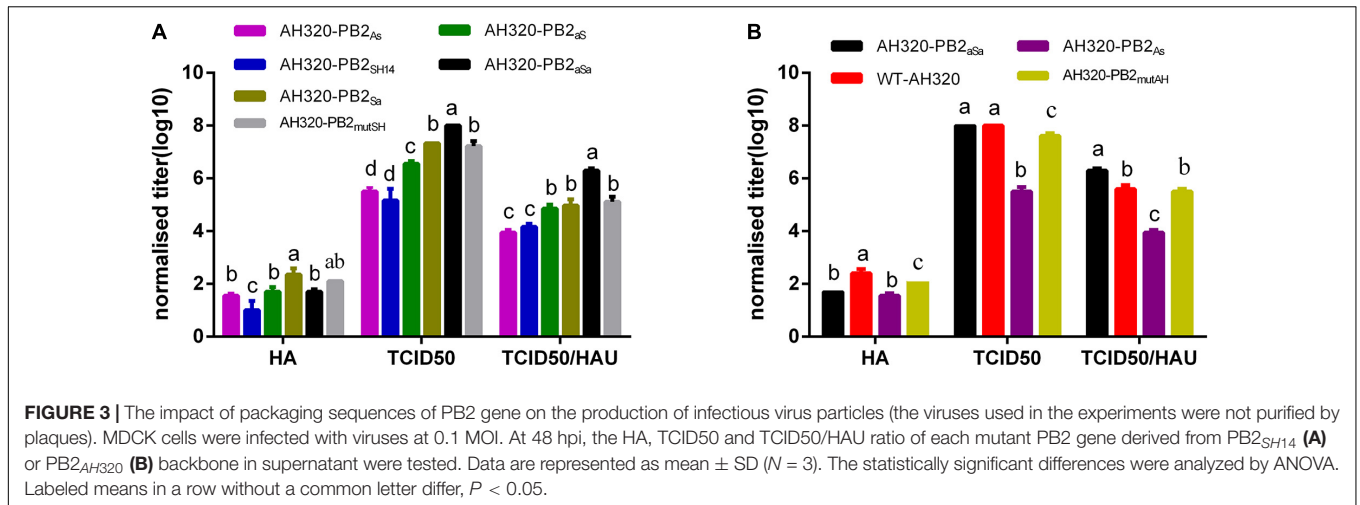


**TABLE 1 |** The infectivity titer (TCID<sub>50</sub>/100  $\mu$ l) and Total titer (HA/25  $\mu$ l) change between the viruses allantoic fluid before and after purifying by series plaque.

Viruses	Allantoic fluid of rescued viruses			Allantoic fluid of plaque purified viruses		
	Infectivity titer (TCID <sub>50</sub> /100 $\mu$ l)	Total titer (HA/25 $\mu$ l)	TCID <sub>50</sub> /HAU	Infectivity titer (TCID <sub>50</sub> /100 $\mu$ l)	Total titer (HA/25 $\mu$ l)	TCID <sub>50</sub> /HAU
WT-AH320	6.5	8	12,352	8.5	11	154,408
AH320-PB2 <sub>AS</sub>	5.625	9.5	582	8.5	11	154,408
AH320-PB2 <sub>mutAH</sub>	6.5	8.5	8,734	8.33	10.5	147,633
AH320-PB2 <sub>SH14</sub>	4.5	8.5	87	8.0	11	48,828
AH320-PB2 <sub>Sa</sub>	5.167	8.5	405	7.67	10	45,677
AH320-PB2 <sub>aS</sub>	5.33	8	835	8.5	11	154,408
AH320-PB2 <sub>aSa</sub>	5	7	781	7.5	9	61,763
AH320-PB2 <sub>mutSH</sub>	5.5	8.5	873	8	11	48,828



increased virus replication to the level comparable to P-WT-AH320 virus (Figures 4A,B). Reciprocally, substitution of the packaging region at 3' end of PB2<sub>AH320</sub> lowered the rate of P-AH320-PB2<sub>AS</sub> virus replication to a level similar

to P-AH320-PB2<sub>SH14</sub> (Figure 4B). However, alteration of amino acids at position 44 and 676 of either PB2<sub>SH14</sub> or PB2<sub>AH320</sub> had little effect on the replication of H9N2 viruses (Figures 4C,D). Similar observations were made

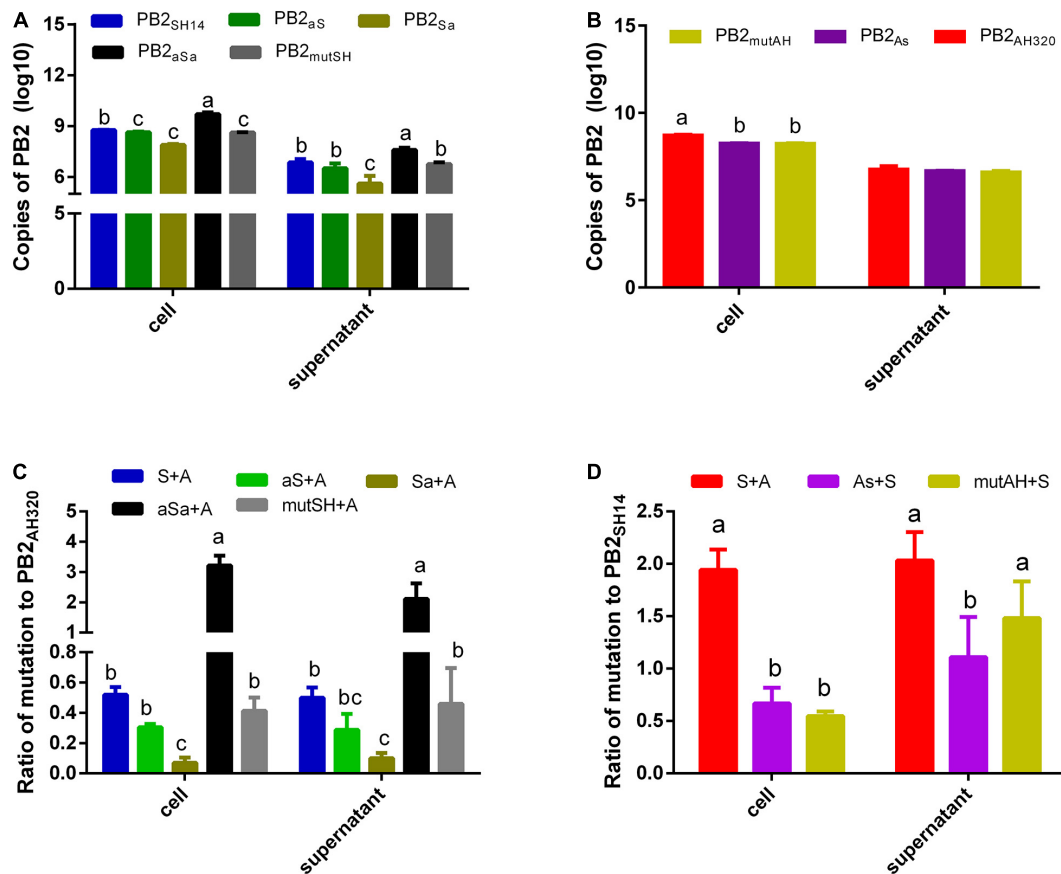


**FIGURE 5** | MDCK cells were infected (A,B) or coinfecting (C,D) with plaque purified viruses at 1 MOI. And an inhibitor of endosome acidification, ammonium chloride was added to restrict the infection to a single cycle. At 48 hpi, the copy number of each PB2 gene in infected cells and supernatants was detected by real-time RT-QPCR. And the ratios to PB2<sub>AH320</sub>/PB2<sub>SH14</sub> of each mutant PB2 gene derived from PB2<sub>SH14</sub>/PB2<sub>AH320</sub> backbone were calculated in coinfection groups (C,D). S, P-AH320-PB2<sub>SH14</sub>; aS, P-AH320-PB2<sub>aS</sub>; Sa, P-AH320-PB2<sub>Sa</sub>; aSa, P-AH320-PB2<sub>aSa</sub>; mutSH, P-AH320-PB2<sub>mutSH</sub>; A, P-WT-AH320; As, P-AH320-PB2<sub>As</sub>; mutAH, P-AH320-PB2<sub>mutAH</sub> in (C,D). Data represent the mean  $\pm$  SD from six independent infections. The statistically significant differences were analyzed by ANOVA. Labeled means in a row without a common letter differ,  $P < 0.05$ .

with the use of CEF cells as well as in MDCK cells (Supplementary Figure 2).

## Packaging Regions of PB2 Are Involved in Competitive Advantage in Co-infection

The copy number of PB2<sub>SH14</sub> gene was significantly higher than that of PB2<sub>aSa</sub> vRNA but lower than that of PB2<sub>Sa</sub> vRNA in the cell lysates and conditioned media of MDCK cells infected with 1 MOI of reassortant virus (Figure 5A). While vRNA of PB2<sub>aS</sub> and PB2<sub>mutSH</sub> accumulated comparable copies with that of PB2<sub>SH14</sub> gene in cells and supernatants (Figure 5A). Substitution of packaging sequences at 3' end or amino acid mutation at 44 and 676 positions in PB2<sub>AH320</sub> resulted in a moderate reduction of the copy number of PB2 vRNA in infected cells, but had little impact on the number of PB2 copies in the infected supernatant (Figure 5B).

When co-infected with P-WT-AH320, the ratio of PB2<sub>SH14</sub>/PB2<sub>AH320</sub> copy number was approximately 0.52 in co-infected cells and 0.50 in the conditioned media. Replacing the

packaging regions of PB2<sub>SH14</sub> at two ends with that of PB2<sub>AH320</sub> sequences (P-AH320-PB2<sub>aSa</sub> virus) further increased this ratio in the co-infected cells and conditioned media (Figure 5C). In contrast, the ratios of PB2<sub>aS</sub>/PB2<sub>AH320</sub> and PB2<sub>Sa</sub>/PB2<sub>AH320</sub> copy number decreased in both the virus-infected cells and conditioned media. Amino acid alterations at position 44 and 676 in PB2<sub>SH14</sub> had little effect on its competition advantage. Reciprocally, replacing the 3'-terminal packaging region of PB2<sub>AH320</sub> with the F98-like sequences from PB2<sub>SH14</sub> (P-AH320-PB2<sub>aS</sub>) reduced PB2<sub>aS</sub>/PB2<sub>SH14</sub> ratio in the co-infected cells and conditioned media (Figure 5D). Substitution of two amino acids in PB2<sub>AH320</sub> decreased the number of PB2<sub>mutAH</sub> copy in the cells but not in the conditioned media.

## The Packaging Regions of G1-Like PB2 Extend the Lengths of Virus Shedding

The P-WT-AH320 virus produced significantly higher titers in lungs than did the reassortant virus carrying the PB2<sub>SH14</sub> segment (P-AH320-PB2<sub>SH14</sub>) at 5 dpi (Figure 6A). Viruses were

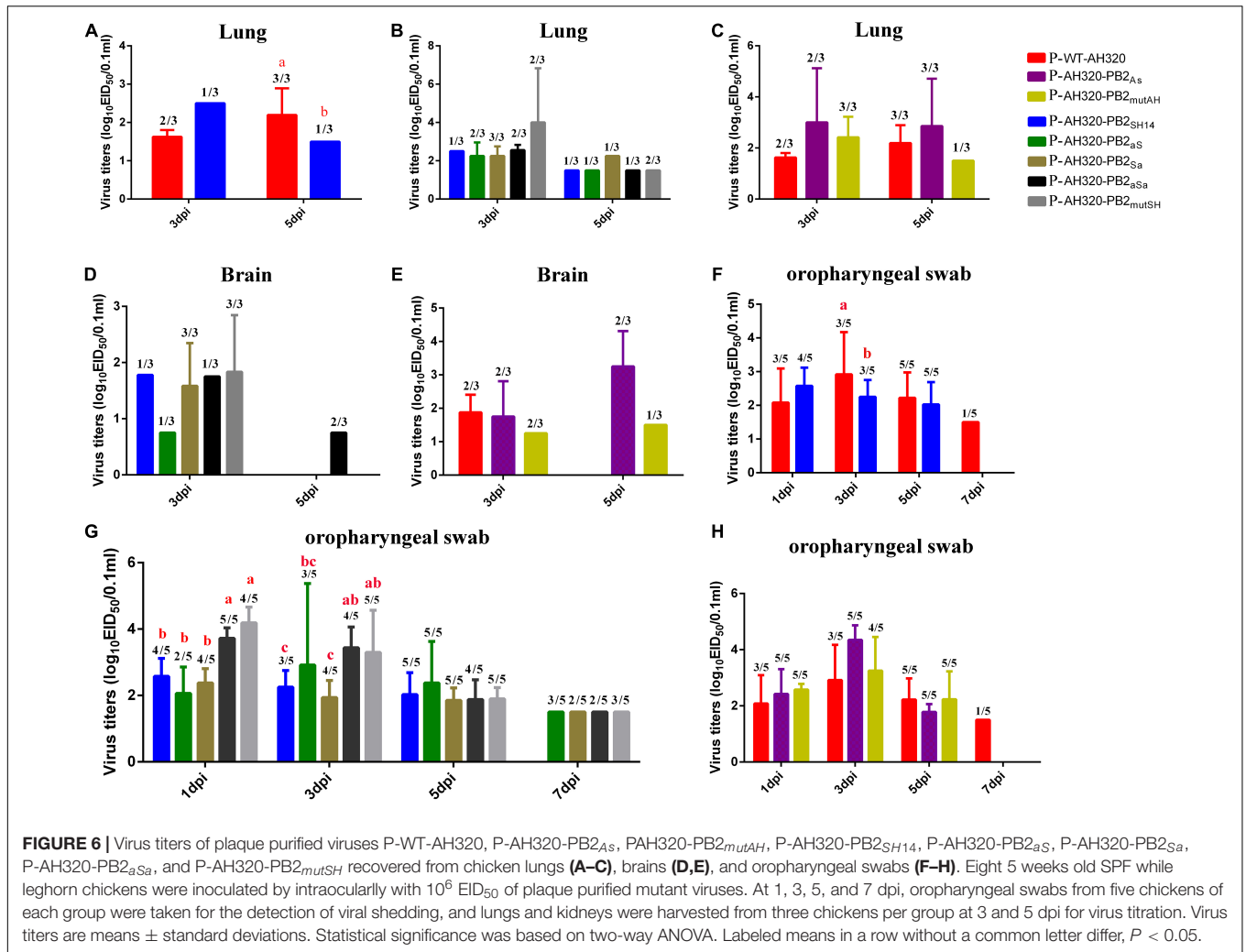


**TABLE 2 |** Virus shedding for the inoculated chickens infected with the reassortant H9N2 viruses.

Strains	1 dpi	3 dpi	5 dpi	7 dpi
	CL	CL	CL	CL
WT-AH320	1.5 ± 0 (1/5)	1.50 ± 0 (1/5)	1.50 ± 0 (3/5)	ND
AH320-PB2 <sub>AS</sub>	1.25 ± 0.35 (3/5)	2.00 ± 0.50 (4/5)	2.19 ± 0.41 (4/5)	ND
AH320-PB2 <sub>mutAH</sub>	ND	2.00 ± 0.54 (3/5)	2.38 ± 0.88 (4/5)	ND
AH320-PB2 <sub>SH14</sub>	ND	ND	1.5 ± 0 (2/5)	ND
AH320-PB2 <sub>aS</sub>	1.13 ± 0.38 (2/5)	1.50 ± 0 (3/5)	1.56 ± 0.11 (4/5)	ND
AH320-PB2 <sub>Sa</sub>	ND	1.50 ± 0 (2/5)	ND	ND
AH320-PB2 <sub>aSa</sub>	ND	1.50 ± 0 (2/5)	1.69 ± 0.32 (4/5)	ND
AH320-PB2 <sub>mutSH</sub>	ND	3.33 ± 0.59 (3/5)	2.33 ± 1.01 (3/5)	ND

Five 5 weeks old SPF chickens were inoculated with 10<sup>6</sup> EID<sub>50</sub> of the H9N2 viruses in a volume of 0.1 ml, respectively. At 1, 3, 5, and 7 dpi, cloacal swabs were taken and suspended in 1 ml of PBS, for the detection of virus shedding in eggs. dpi, day post-inoculation; CL, cloacal swab.

detected in the lungs (Figure 6B) and brain (Figure 6D) in one of three chickens infected with the P-AH320-PB2<sub>SH14</sub> virus at 3 and 5 dpi. The number of chickens tested positive in lungs for the mutant virus that replacing the packaging regions of PB2<sub>SH14</sub> with that of PB2<sub>AH320</sub> gene increased at 3 dpi (Figure 6B). And

a similar increased number of chickens tested positive for the mutant virus in brains were observed (Figure 6D). However, substituting the packaging regions of PB2<sub>AH320</sub> with the F98-like sequences had little influence on the viral load in lungs or brains (Figures 6C,E).

At 7 dpi, the P-WT-AH320 virus could still be detected in one of five chickens from the oropharyngeal swabs, while the P-AH320-PB2<sub>SH14</sub> virus shedding from the trachea only lasted for 5 days (Figure 6F). Virus loads were significantly higher in the trachea of chickens infected with P-AH320-PB2<sub>aSa</sub>, and P-AH320-PB2<sub>mutSH</sub> at 1 and 3 dpi than their parental P-AH320-PB2<sub>SH14</sub> virus (Figure 6G). All mutant viruses remained detectable in oropharyngeal swabs at 7 dpi (Figure 6G). On the contrary, the tracheal shedding of the mutants P-AH320-PB2<sub>As</sub> and P-AH320-PB2<sub>mutAH</sub> was curtailed to 5 days (Figure 6H).

Viruses were detectable in cloacal swabs from chickens infected with the P-WT-AH320 virus at 1, 3, 5 dpi but not detectable in those infected with the P-AH320-PB2<sub>SH14</sub> virus until at 5 dpi (Table 2). However, viruses were detected at 1, 3, and 5 dpi in cloacal swabs from chickens infected with the viruses replacing the packaging regions of PB2<sub>SH14</sub> with the G1-like sequences of PB2<sub>AH320</sub> (the AH320-PB2<sub>aS</sub>, AH320-PB2<sub>aSa</sub>, AH320-PB2<sub>aSa</sub>, and AH320-PB2<sub>mutSH</sub> viruses, Table 2).

## DISCUSSION

Codon usage is crucial for translational elongation efficiency and protein folding (Sabi and Tuller, 2014). Synonymous codons are biasedly used by a variety of microbes (Sharp et al., 1988; Plotkin and Kudla, 2011). Our present study shows that the amino acid sequences of the PB2 gene among the five independent branches were relatively conserved, but their nucleotide sequences were variable (Supplementary Table 1). This suggests the presence of a large number of synonymous codons in the PB2 gene. Nucleotide variations between F98-like and G1-like PB2 genes are likely to produce different RNA structures that affect mRNA splicing, protein translation, vRNA packaging, and influenza A virus replication (Kobayashi et al., 2016; Spronken et al., 2017; Baranovskaya et al., 2019).

There is growing evidence that packaging signals play important roles in virus replication, genome incorporation, and genetic reassortment of influenza A virus (Gao and Palese, 2009; Essere et al., 2013; Gerber et al., 2014). Substitutions of the packaging regions of PB2<sub>SH14</sub> and PB2<sub>AH320</sub> genes significantly affected the protein expression and RNA synthesis of the PB2 segment. Moreover, the proportion of infectious virus particles were elevated by substituting the packaging regions of F98-like PB2 gene with the G1-like sequences relative to their parental AH320-PB2<sub>SH14</sub> virus.

Our study also showed that replacing the both ends packaging regions of PB2<sub>SH14</sub> with the PB2<sub>AH320</sub> sequences enhanced its copy number ratio in co-infections, whereas, replacing 3' or 5' end packaging region decreased this ratio. One explanation is that different nucleotide sequences in the packaging regions between PB2<sub>SH14</sub> and PB2<sub>AH320</sub> leads to different RNA structures or interactions among segments. Previous studies have shown that different segments of influenza virus acquire unique RNA conformations and form RNA interactions between intra- and intersegment inside virions (Dadonaite et al., 2019). The variation of vRNA structure may have a great impact on the genome packaging, replication and reassortment of influenza virus

(Fournier et al., 2012; Gavazzi et al., 2013; Gerber et al., 2014; Shafiuddin and Boon, 2019). Another explanation is that the internal coding regions of PB2 harbor an unknown packaging sequence, as suggested by recent studies showing that the internal coding regions of the PB1 gene also play an important role in the packaging of influenza A virus genome (Liang et al., 2005; Muramoto et al., 2006; Gilbertson et al., 2016). In support of this notion, we found that amino acid alterations at position 44 and 676 of PB2<sub>AH320</sub> decreased the ratio of PB2<sub>mutAH</sub>/PB2<sub>SH14</sub> copy number in co-infected cells (Figure 5D) but did not affect this ratio in the viruses in the conditioned media. This result indicates that in complex coinfection conditions, the amino acid mutation reduced vRNA replication of PB2<sub>mutAH</sub>, but did not influence its competitive advantage at incorporation stage.

*In vitro* cell culture experiments revealed that the packaging regions of G1-like PB2 increased virus replication. However, the packaging regions of G1-like PB2 only modestly enhanced virus replication in chickens but pronouncing extended the length of virus shedding time and the odds of virus detection in trachea and cloacae. These results suggest that viruses harboring PB2 genes with the G1-like packaging sequences produce more infectious virus particles, leading to the dominance of H9N2 virus in circulation.

Influenza virus reassortment is controlled by many factors such as compatibility among polymerase subunits and segments mismatch (Marshall et al., 2013; White and Lowen, 2018). Most reassortment events lead to incompatibilities at protein and vRNA levels, resulting in the production of defective virions (White and Lowen, 2018). The persistent epidemics of genotype S H9N2 virus in China implies the high compatibility among its vRNA segments.

In summary, our study has demonstrated that the packaging sequences of G1-like PB2 enhanced the production of infectious viral particles of H9N2 virus *in vitro* and *in vivo*. Replacing the packaging regions of F98-like PB2 at both ends with the G1-like sequences further enhance the competitive advantages of virus replication. Our study suggests that H9N2 viruses acquire replication advantages by optimizing their PB2 nucleotide sequences.

## DATA AVAILABILITY STATEMENT

Publicly available datasets were analyzed in this study. The data presented in the study are deposited in the EpiFlu Database (GISAID): <https://www.gisaid.org/registration/terms-of-use/>. The isolate IDs can be found in **Supplementary Dataset 1**. The datasets generated and analyzed during this current study are available from the corresponding author.

## ETHICS STATEMENT

The animal study was reviewed and approved by the Jiangsu Administrative Committee for Laboratory Animals (Permission number: SYXK-SU-2017-0007), the Institutional Biosafety Committee of Yangzhou University, and Jiangsu laboratory

animal welfare and ethics of Jiangsu Administrative Committee of Laboratory Animals.

## AUTHOR CONTRIBUTIONS

XLL and MG designed this study. XLL, YZ, SQ, RG, ZG, and JM performed the experiments. XLL, MG, XX, XW, JH, SH, XLW, SC, DP, XJ, and XFL drafted and revised the manuscript. All authors read and approved the final manuscript.

## FUNDING

This work was supported by the National Natural Science Foundation of China (31702245), the Jiangsu Provincial Natural Science Fund for Excellent Young Scholars (BK20170068), the National Key Research and Development project of China (2016YFD0500202), the Earmarked fund for China Agriculture Research System (CARS-40), the Priority Academic Program

## REFERENCES

- Baranovskaya, I., Sergeeva, M., Fadeev, A., Kadirova, R., Ivanova, A., Ramsay, E., et al. (2019). Changes in RNA secondary structure affect NS1 protein expression during early stage influenza virus infection. *Viol. J.* 16:162.
- Bolte, H., Rosu, M. E., Hagelauer, E., García-Sastre, A., and Schwemmler, M. (2019). Packaging of the influenza virus genome is governed by a plastic network of RNA- and nucleoprotein-mediated interactions. *J. Virol.* 93:e01861-18.
- Carter, M. J., and Mahy, B. W. (1982a). Incomplete avian influenza virus contains a defective non-interfering component. *Arch. Virol.* 71, 13–25.
- Carter, M. J., and Mahy, B. W. (1982b). Synthesis of RNA segments 1-3 during generation of incomplete influenza A (fowl plague) virus. *Arch. Virol.* 73, 109–119.
- Chen, G., Gharib, T. G., Huang, C. C., Taylor, J. M., Misk, D. E., Kardias, S. L., et al. (2002). Discordant protein and mRNA expression in lung adenocarcinomas. *Mol. Cell. Proteomics* 1, 304–313.
- Cobbin, J. C., Ong, C., Verity, E., Gilbertson, B. P., Rockman, S. P., and Brown, L. E. (2014). Influenza virus PB1 and neuraminidase gene segments can cosegregate during vaccine reassortment driven by interactions in the PB1 coding region. *J. Virol.* 88, 8971–8980.
- Dadonaite, B., Gilbertson, B., Knight, M. L., Trifkovic, S., Rockman, S., Laederach, A., et al. (2019). The structure of the influenza A virus genome. *Nat. Microbiol.* 4, 1781–1789.
- Essere, B., Yver, M., Gavazzi, C., Terrier, O., Isel, C., Fournier, E., et al. (2013). Critical role of segment-specific packaging signals in genetic reassortment of influenza A viruses. *Proc. Natl. Acad. Sci. U.S.A.* 110, E3840–E3848.
- Fournier, E., Moules, V., Essere, B., Paillart, J. C., Sirbat, J. D., Isel, C., et al. (2012). A supramolecular assembly formed by influenza A virus genomic RNA segments. *Nucleic Acids Res.* 40, 2197–2209.
- Gao, Q., and Palese, P. (2009). Rewriting the RNAs of influenza virus to prevent reassortment. *Proc. Natl. Acad. Sci. U.S.A.* 106, 15891–15896.
- Gavazzi, C., Yver, M., Isel, C., Smyth, R. P., Rosa-Calatrava, M., Lina, B., et al. (2013). A functional sequence-specific interaction between influenza A virus genomic RNA segments. *Proc. Natl. Acad. Sci. U.S.A.* 110, 16604–16609.
- Gerber, M., Isel, C., Moules, V., and Marquet, R. (2014). Selective packaging of the influenza A genome and consequences for genetic reassortment. *Trends Microbiol.* 22, 446–455.
- Gilbertson, B., Zheng, T., Gerber, M., Printz-Schweigert, A., Ong, C., Marquet, R., et al. (2016). Influenza NA and PB1 gene segments interact during the formation of viral progeny: localization of the binding region within the PB1 Gene. *Viruses* 8:238.

Development of Jiangsu Higher Education Institutions (PAPD), the Jiangsu Qinglan project and the “high-end talent support program” of Yangzhou University.

## SUPPLEMENTARY MATERIAL

The Supplementary Material for this article can be found online at: <https://www.frontiersin.org/articles/10.3389/fmicb.2021.655057/full#supplementary-material>

**Supplementary Figure 1** | Phylogenetic trees of PB2 gene segments of the H9N2 viruses during 1996–2019 isolated in China.

**Supplementary Figure 2** | Multiple-cycle growth curves of plaque purified H9N2 viruses in CEF cells. The replication abilities of each virus in CEF cells was measured by infecting cells at an MOI of 0.1. Virus titers in supernatant were determined in CEF cells at indicated time points. Data are represented as mean  $\pm$  SD ( $N = 3$ ). The statistically significant differences were analyzed by ANOVA compared with P-AH320-PB2<sub>SH14</sub> or P-WT-AH320 virus (\* $P < 0.05$ ; \*\* $P < 0.01$ ; \*\*\* $P < 0.001$ ).

- Griffin, T. J., Gygi, S. P., Ideker, T., Rist, B., Eng, J., Hood, L., et al. (2002). Complementary profiling of gene expression at the transcriptome and proteome levels in *Saccharomyces cerevisiae*. *Mol. Cell. Proteomics* 1, 323–333.
- Gu, M., Chen, H., Li, Q., Huang, J., Zhao, M., Gu, X., et al. (2014). Enzootic genotype S of H9N2 avian influenza viruses donates internal genes to emerging zoonotic influenza viruses in China. *Vet. Microbiol.* 174, 309–315.
- Gu, M., Xu, L., Wang, X., and Liu, X. (2017). Current situation of H9N2 subtype avian influenza in China. *Vet. Res.* 48:49.
- Hao, X., Hu, J., Wang, X., Gu, M., Wang, J., Liu, D., et al. (2020). The PB2 and M genes are critical for the superiority of genotype S H9N2 virus to genotype H in optimizing viral fitness of H5Nx and H7N9 avian influenza viruses in mice. *Transbound. Emerg. Dis.* 67, 758–768.
- Hao, X., Wang, X., Hu, J., Gu, M., Wang, J., Deng, Y., et al. (2019). The PB2 and M genes of genotype S H9N2 virus contribute to the enhanced fitness of H5Nx and H7N9 avian influenza viruses in chickens. *Virology* 535, 218–226.
- Huang, Y., Hu, B., Wen, X., Cao, S., Gavrillov, B. K., Du, Q., et al. (2010). Diversified reassortant H9N2 avian influenza viruses in chicken flocks in northern and eastern China. *Virus Res.* 151, 26–32.
- Kobayashi, Y., Dadonaite, B., van Doremalen, N., Suzuki, Y., Barclay, W. S., and Pybus, O. G. (2016). Computational and molecular analysis of conserved influenza A virus RNA secondary structures involved in infectious virion production. *RNA Biol.* 13, 883–894.
- Kobayashi, Y., Pybus, O. G., Itou, T., and Suzuki, Y. (2018). Conserved secondary structures predicted within the 5′ packaging signal region of influenza A virus PB2 segment. *Meta Gene* 15, 75–79.
- Li, C., Wang, S., Bing, G., Carter, R. A., Wang, Z., Wang, J., et al. (2017). Genetic evolution of influenza H9N2 viruses isolated from various hosts in China from 1994 to 2013. *Emerg. Microbes Infect.* 6:e106.
- Liang, Y., Hong, Y., and Parslow, T. G. (2005). cis-Acting packaging signals in the influenza virus PB1, PB2, and PA genomic RNA segments. *J. Virol.* 79, 10348–10355.
- Liang, Y., Huang, T., Ly, H., Parslow, T. G., and Liang, Y. (2008). Mutational analyses of packaging signals in influenza virus PA, PB1, and PB2 genomic RNA segments. *J. Virol.* 82, 229–236.
- Liu, Y. F., Lai, H. Z., Li, L., Liu, Y. P., Zhang, W. Y., Gao, R., et al. (2016). Endemic variation of H9N2 avian influenza virus in China. *Avian Dis.* 60, 817–825.
- Marjuki, H., Yen, H. L., Franks, J., Webster, R. G., Pleschka, S., and Hoffmann, E. (2007). Higher polymerase activity of a human influenza virus enhances activation of the hemagglutinin-induced Raf/MEK/ERK signal cascade. *Viol. J.* 4:134.

- Marshall, N., Priyamvada, L., Ende, Z., Steel, J., and Lowen, A. C. (2013). Influenza virus reassortment occurs with high frequency in the absence of segment mismatch. *PLoS Pathog.* 9:e1003421. doi: 10.1371/journal.ppat.1003421
- McAuley, J. L., Zhang, K., and McCullers, J. A. (2010). The effects of influenza A virus PB1-F2 protein on polymerase activity are strain specific and do not impact pathogenesis. *J. Virol.* 84, 558–564.
- Muramoto, Y., Takada, A., Fujii, K., Noda, T., Iwatsuki-Horimoto, K., Watanabe, S., et al. (2006). Hierarchy among viral RNA (vRNA) segments in their role in vRNA incorporation into influenza A virions. *J. Virol.* 80, 2318–2325.
- Ozawa, M., Maeda, J., Iwatsuki-Horimoto, K., Watanabe, S., Goto, H., Horimoto, T., et al. (2009). Nucleotide sequence requirements at the 5' end of the influenza A virus M RNA segment for efficient virus replication. *J. Virol.* 83, 3384–3388.
- Plotkin, J. B., and Kudla, G. (2011). Synonymous but not the same: the causes and consequences of codon bias. *Nat. Rev. Genet.* 12, 32–42.
- Sabi, R., and Tuller, T. (2014). Modelling the efficiency of codon-tRNA interactions based on codon usage bias. *DNA Res.* 21, 511–526.
- Salomon, R., Franks, J., Govorkova, E. A., Ilyushina, N. A., Yen, H. L., Hulse-Post, D. J., et al. (2006). The polymerase complex genes contribute to the high virulence of the human H5N1 influenza virus isolate A/Vietnam/1203/04. *J. Exp. Med.* 203, 689–697.
- Shafiuddin, M., and Boon, A. C. M. (2019). RNA sequence features are at the core of influenza A virus genome packaging. *J. Mol. Biol.* 431, 4217–4228.
- Sharp, P. M., Cowe, E., Higgins, D. G., Shields, D. C., Wolfe, K. H., and Wright, F. (1988). Codon usage patterns in *Escherichia coli*, *Bacillus subtilis*, *Saccharomyces cerevisiae*, *Schizosaccharomyces pombe*, *Drosophila melanogaster* and *Homo sapiens*; a review of the considerable within-species diversity. *Nucleic Acids Res.* 16, 8207–8211.
- Spronken, M. I., van de Sandt, C. E., de Jongh, E. P., Vuong, O., van der Vliet, S., Bestebroer, T. M., et al. (2017). A compensatory mutagenesis study of a conserved hairpin in the M gene segment of influenza A virus shows its role in virus replication. *RNA Biol.* 14, 1606–1616.
- White, M. C., and Lowen, A. C. (2018). Implications of segment mismatch for influenza A virus evolution. *J. Gen. Virol.* 99, 3–16.
- White, M. C., Steel, J., and Lowen, A. C. (2017). Heterologous packaging signals on segment 4, but not segment 6 or segment 8, limit influenza A virus reassortment. *J. Virol.* 91:e00195-17.
- Xue, J., Chambers, B. S., Hensley, S. E., and López, C. B. (2016). Propagation and characterization of influenza virus stocks that lack high levels of defective viral genomes and hemagglutinin mutations. *Front. Microbiol.* 7:326. doi: 10.3389/fmicb.2016.00326
- Zhang, Y., Yin, Y., Bi, Y., Wang, S., Xu, S., Wang, J., et al. (2012). Molecular and antigenic characterization of H9N2 avian influenza virus isolates from chicken flocks between 1998 and 2007 in China. *Vet. Microbiol.* 156, 285–293.
- Zhao, F. F., Lu, Y. Y., Feng, Y., Xu, C. P., and Mo, S. H. (2011). [Study on the mutations within the whole genome of influenza virus subtype A/H3N2 strains circulated in Zhejiang province from 1998 to 2009]. *Zhonghua Yu Fang Yi Xue Za Zhi* 45, 612–618.
- Zhao, L., Peng, Y., Zhou, K., Cao, M., Wang, J., Wang, X., et al. (2014). New insights into the nonconserved noncoding region of the subtype-determinant hemagglutinin and neuraminidase segments of influenza A viruses. *J. Virol.* 88, 11493–11503.

**Conflict of Interest:** The authors declare that the research was conducted in the absence of any commercial or financial relationships that could be construed as a potential conflict of interest.

Copyright © 2021 Li, Zhao, Qiao, Gu, Gao, Ge, Xu, Wang, Ma, Hu, Hu, Liu, Chen, Peng, Jiao and Liu. This is an open-access article distributed under the terms of the Creative Commons Attribution License (CC BY). The use, distribution or reproduction in other forums is permitted, provided the original author(s) and the copyright owner(s) are credited and that the original publication in this journal is cited, in accordance with accepted academic practice. No use, distribution or reproduction is permitted which does not comply with these terms.